







Influence of anionic surfactant on stability of nanoparticles in aqueous solutions

Dmitry O. Zelentsov ^a , Yuliya Yu. Petrova ^{a*} , Alexander V. Korobkin ^a,
Anastasia A. Ivanova ^b , Alexey N. Cheremisin ^b , Ivan I. Shanenkov ^c ,
Alexander Ya. Pak ^d , Yuliya G. Mateyshina ^e

a: Institute of Natural and Technical Sciences, Surgut State University, Surgut 628408, Russia

b: Skoltech Center for Petroleum Science and Engineering, Skoltech, Moscow 121205, Russia

c: Institute of Environmental and Agricultural Biology, Tyumen State University, Tyumen 625003, Russia

d: School of Energy and Power Engineering, Tomsk Polytechnic University, Tomsk 634050, Russia

e: Institute of Solid State Chemistry and Mechanochemistry, Siberian Branch of the Russian Academy of Sciences, Novosibirsk 630090, Russia

* Corresponding author: petrova_juju@surgu.ru

This paper belongs to the RKFМ'23 Special Issue: <https://chem.conf.nstu.ru/>.

Guest Editors: Prof. N. Uvarov and Prof. E. Aubakirov.

Abstract

Dispersion and aggregation of nanoparticles in aqueous solutions are important factors for safe and effective application of nanoparticles, for instance, in the oil industry. As conventional oil reserves are depleted, it is necessary to advance chemical enhanced oil recovery (cEOR) techniques to develop unconventional oil reservoirs. Nanoparticles modified by surfactants can be a promising reagent in cEOR. These nanomaterials can reduce interfacial tension and change the wettability of reservoir rock, which leads to an increase in oil recovery. However, the application of nanoparticles is limited by their substantial aggregation in aqueous solutions. The purpose of this work is to select nanoparticles for obtaining stable sols in water in the presence of an anionic surfactant and to optimize the conditions (pH) for further modifying the nanoparticles with the anionic surfactant. Sodium dodecyl sulfate (SDS) is used as an anionic surfactant. The aggregation of oxide and carbon nanoparticles in water and anionic surfactant solutions was studied by laser diffraction, dynamic and electrophoretic light scattering methods. Most of the studied nanoparticles in water form aggregates with bi-, three- and polymodal particle size distributions. TiO₂ nanoparticles obtained by plasma dynamic synthesis form the most stable sols in anionic surfactant solutions. The range of 5–7 pH is defined as optimal for their modification with surfactants. The stability of carbon nanoparticles in aqueous solutions increases significantly in the presence of a surfactant. The obtained results form the basis for further research on the modification of marked nanoparticles in surfactant solutions.

Key findings

- TiO₂ nanoparticles form the most stable sols in anionic surfactant solutions.
- 5–7 pH is optimal for modification of TiO₂ with sodium dodecyl sulfate.
- Carbon nanoparticles are significantly more stable in anionic surfactant solutions.

© 2023, the Authors. This article is published in open access under the terms and conditions of the Creative Commons Attribution (CC BY) license (<http://creativecommons.org/licenses/by/4.0/>).

1. Introduction

With the increased attention toward nanotechnology and its innovative use for different industries including, but not

limited to, food, biomedical, electronics, materials, etc., the application of nanotechnology or nanoparticles in the oil and gas industry is a subject undergoing intensive study by major oil companies, which is reflected in the



Keywords

nanoparticles
anionic surfactant
titan oxide
carbon nanoparticles
aggregation

Received: 09.07.23

Revised: 24.07.23

Accepted: 24.07.23

Available online: 27.07.23



huge amount of funds invested in the research and development of nanotechnology. Nanotechnology has been recently investigated extensively for different applications in the oil and gas industry, such as drilling fluids and enhanced oil recovery, in addition to other applications including cementing and well stimulation [1].

As conventional oil reserves are gradually depleted, oil producers are increasingly seeking to develop oil reservoirs that have already been discovered. Developing oil reservoirs characterized by high temperatures and ultra-low permeability is becoming a major challenge. This can be handled by using chemical enhanced oil recovery (cEOR) techniques. They receive a great deal of attention because they allow controlling the properties at the oil-fluid and oil-rock interfaces. Nanotechnology applications in cEOR are studied by researchers around the world [2–5]. First of all, nanoparticles (NPs) can adsorb on reservoir rock and change its wettability from oil-wet to water-wet [6–7]. Also, nanoparticles can adsorb at the oil-fluid interface and reduce the interfacial tension, which also leads to an increase in oil displacement [8].

A limitation in the application of NPs is their low stability in liquid systems and tendency to aggregation [9]. At high mineralization and high temperatures, aggregation of nanoparticles may increase even more. Flooding a reservoir with fluids containing large aggregates of NPs may lead to clogging of small reservoir pores, which will have a negative effect on the overall oil recovery [10].

To prevent excessive aggregation of NPs, they are modified with surfactants. The modification is carried out by two methods: in-situ (physical adsorption) and ex-situ (chemical grafting) [11]. The obtained nano-surfactant composites acquire greater surface activity, and their stability in aqueous systems is improved [12]. Fluids with modified NPs were shown to displace oil more effectively [13]. Adsorbed surfactant molecules can prevent excessive aggregation of NPs, but the opposite effect is also possible [14]. It was noted that dispersions with smaller aggregates of nanoparticles are more effective in reducing the interfacial tension [13, 15], and the efficiency in the wettability alteration of modified NPs is higher than that of unmodified ones or surfactant solutions without NPs [16–17]. In the work [18] it was shown that modified SiO_2 NPs reduced the adsorption of surfactants on the rock. Modification conditions, such as the type of nanoparticles and a surfactant, the ratio of their concentrations, pH and mineralization, can significantly affect the efficiency of modified nanoparticles in oil displacement [19–23].

In this work, we selected nanoparticles that form the most stable dispersions or sols in water and anionic surfactant solutions. Also, for the selected nanoparticles we studied the effect of pH on their aggregation in surfactant solution to choose the optimal conditions for further modifying NPs with the surfactant.

2. Materials and Methods

2.1. Materials

The following silica and titanium oxide NPs (Sigma-Aldrich) were used in this work: SiO_2 and TiO_2 -SA; β - Bi_2O_3 NPs obtained by thermal decomposition of $\text{BiC}_2\text{H}_4(\text{OH})$ [24]; graphite-like carbon nanoparticles (C-NPs) obtained by plasma treatment of asphaltenes [25]; and NPs obtained by plasma dynamic synthesis [26]: titanium oxides (TiO_2 – particles containing magnelli-phase with a wide size distribution from 1 nm to 50 μm , TiO_2 -BK – fine particles up to 1 μm in size), aluminum oxide and a mixture of iron oxides. Sodium dodecyl sulfate (SDS, PanReac) was used as an anionic surfactant. Sodium hydroxide (LenReactiv, >99%), phosphoric acid (Component-Reaktiv, >99%), and phosphate buffer solutions prepared from disodium hydrogen phosphate (Merck, >99.9%) and sodium dihydrogen phosphate 2-hydrate (Merck, >99.9%) were used to adjust pH.

2.2. Nanoparticle characterization

The physical-chemical characterization was done using the X-ray fluorescence (vacuum 8–12 Pa, energy-dispersive analyzer EDX-8000, Shimadzu), FT-IR (ATR and transmission mode, Spectrum 100 Series, Perkin Elmer) and TGA/DSC analysis. The TGA/DSC analysis of the nanoparticles was performed with a Mettler Toledo TGA/DSC 3+ Star System, at a heating rate of 20 $^\circ\text{C}/\text{min}$, under nitrogen atmosphere with a flow rate of 50 mL/min.

2.3. Size distribution of nanoparticle aggregates by laser diffraction

The particle size was evaluated with a SALD-2300 (Shimadzu) analyzer for selection of oxide nanoparticles and study of surfactant influence on carbon nanoparticle aggregation.

The oxide nanoparticles (~2 mg) were dispersed in 10 ml of distilled water. Before each measurement, the nanofluid sample was sonicated using a probe type sonicator at a frequency of 35 kHz for 10 min. 0.5 ml of the dispersion was taken and placed in a SALD-2300 (Shimadzu) analyzer cuvette filled with 9.5 ml of distilled water or 5, 10, or 50 mmol/L SDS solution, a stirrer was turned on, and particle size measurements were performed for 1 h.

To study the size distribution of C-NPs aggregates, 0.01% dispersions were prepared in water or 5 and 50 mmol/L SDS solutions.

2.4. Zeta-potential and size distribution of NPs by dynamic light scattering

Zeta-potential (ζ) and size distribution of NPs in the nanofluid were measured using a particle size analyser (Litesizer 500, Anton Paar) which works on the principle of dynamic light scattering (DLS) to study the influence of pH on the aggregation of β - Bi_2O_3 and TiO_2 NPs in 5 mmol/L SDS solutions. The solutions were prepared using a phosphate buffer for pH 4.5–9.0, $3.3 \cdot 10^{-4}$ – 3.3 mol/L H_3PO_4 for

pH < 4.0, and 0.25–25 mmol/L NaOH for pH > 9.0. Thus, 0.025% dispersion of NPTs was mixed with a buffer solution (H₃PO₄ or NaOH) and 25 mmol/L SDS in a volume ratio of 2:2:1. The mixture was stirred, and the DLS measurements were performed.

2.5. Interfacial tension (IFT) measurements

IFT measurements between *n*-hexane and different aqueous solutions of nanoparticles were conducted using the spinning drop method (SDT, Kruss, Germany) as it is more convenient and accurate for measuring IFT below 20 mN·m⁻¹ [27]. Here, a drop of liquid with lower density (*n*-hexane) was placed inside the denser fluid (surfactant or surfactant–nanoparticle solutions) in a horizontal tube. Then, the tube was rotated, and the drop deformed into an elongated shape. The samples were assumed to be equilibrated when the measured IFT values remained unchanged (2%) for 30 min [28]. At the equilibrium point, the balance between surface tension and centrifugal forces defined the shape of the droplet. At a high angular velocity ω (max. 15,000 rpm), the droplet shape becomes very close to a cylinder. In this case, the IFT values were calculated using the Vonnegut expression (Equation 1).

$$\sigma = \frac{\Delta\rho\omega^2R^3}{4}, \quad (1)$$

where $\Delta\rho$ is the density difference between light and heavy phases (*n*-hexane and surfactant–nanoparticles formulations, measured with an areometer), and R is the shape radius.

To avoid the influence of impurities on the results, before and after each experiment, the tube was cleaned with acetone and water and then dried with air.

3. Results and Discussion

3.1. Nanoparticle characterization

TiO₂ and carbon NPTs were measured by X-ray fluorescence (XRF), and the results are listed in Table 1.

TiO₂ NPTs obtained by plasma dynamic synthesis contain impurities of iron, silicon, aluminum, calcium, etc., and carbon NPTs obtained by plasma treatment of asphaltenes contain impurities of sulfur.

The FTIR spectrum of TiO₂ NPTs recorded in attenuated total reflection (ATR) mode, shown in Figure 1a, provided additional information about the TiO₂ structure. It can be observed that the strong band in the range of 480 to 660 cm⁻¹ was assigned to Ti–O stretching bands [29]. FTIR absorption spectra of TiO₂ NPTs contain the band (wide peak or shoulder) at approximately around 3500 cm⁻¹ (stretching) which stipulates the presence of hydroxyl groups. The 1635 cm⁻¹ absorption band may be related to hydroxyl (bending) representing the water as moisture in the sample.

The transmission IR spectra of C-NPTs samples synthesized in plasma are presented in Figure 1b. The band at

1600 cm⁻¹ is due to C=C stretching of the aromatic ring. The wide band at 3300–3650 cm⁻¹ can be observed in the spectra due to OH groups.

The differential thermal analysis of TiO₂ NPTs obtained by plasma dynamic synthesis (Figure 2) showed that up to 600 °C, the studied sample was thermally stable (TGA). Upon further increase in temperature above 600 °C in an inert medium, an increase in the sample mass was observed (DTA, maxima at 650 and 850 °C), which can be explained by the formation of nitrides of iron and calcium impurities. At the same time, the wide exothermic peak observed at about 400–650 °C was attributed to the phase transformation from anatase to rutile (DSC).

3.2. Selection of nanoparticles

The next stage of our work was the selection of nanoparticles that form stable sols in SDS solutions. At this stage, we studied the aggregation of oxide nanoparticles by laser diffraction.

SiO₂ NPTs formed large aggregates both in water and in SDS solutions (Figure S1). Thus, the modal size of SiO₂ aggregates in water in 30 min was ~100 μm. Addition of SiO₂ NPTs in SDS solutions led to the formation of smaller aggregates (60~70 μm), which are still large for use in low-permeability reservoirs.

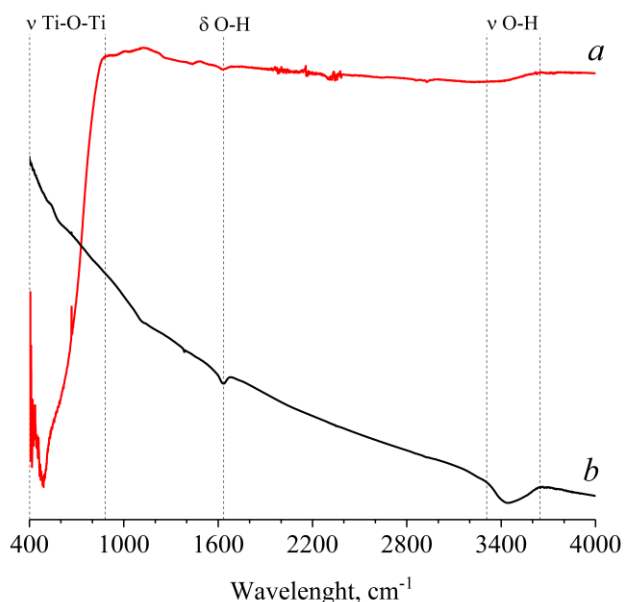
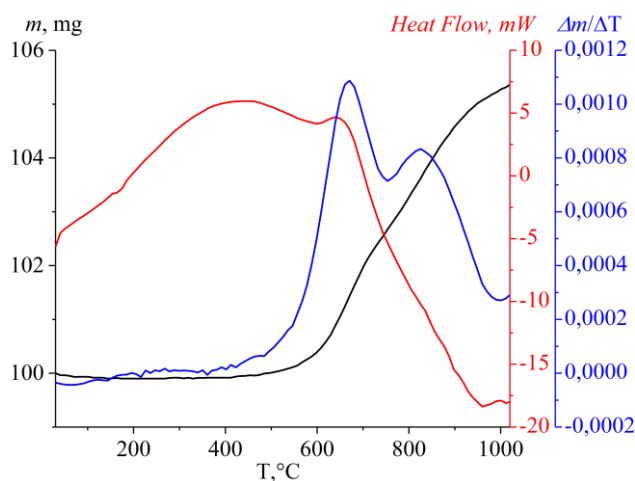
Smaller particle sizes were observed for TiO₂-SA NPTs (Figure S2). In water, the nanoparticles mainly form an aggregate fraction with sizes of ~32 μm in 30 min (Figure S2, a). In 10 and 50 mmol/L surfactant solutions TiO₂-SA aggregation increases, forming aggregates ~127 and ~71 μm (Figure S2, c and d), respectively. And only 5 mmol/L SDS solution has a stabilizing effect, and the bulk of the aggregates form a fraction with a size of ~4 μm (Figure S2, b). This phenomenon can be explained by the fact that in 5 mmol/L solution the surfactant is only partially adsorbed on the surface of NPTs and thus prevents further aggregation of the particles. In 10 mmol/L solution, SDS (or its micelles) is completely adsorbed, or close to it, on the surface of NPTs, forming a monolayer of surfactant molecules. This leads to a sharp increase in the hydrophobicity of the NPTs, which, in turn, leads to an increase in aggregation. And in 50 mmol/L solution, SDS micelles continue to adsorb, forming a bilayer of surfactant molecules. The surface of NPTs becomes more hydrophilic, and the size of the aggregates decreases.

The following is a discussion of nanoparticles of iron, aluminum and titanium oxides obtained by the plasma dynamic synthesis. It should be understood that these nanoparticles are not homogeneous and are a mixture of different oxides. Thus, Fe₂O₃ includes a mixture of magnetite, hematite and ε-Fe₂O₃. Al₂O₃ includes γ-Al₂O₃ and spinel phases. TiO₂ consists not only of rutile and anatase, but also of magnelli phases – non-stoichiometric titanium oxides. The heterogeneous composition can affect the obtained results of particle size distributions.

Table 1 The results of XRF analysis of TiO₂ and carbon NPTs.

Sample	Element, wt. %										
	Ti	O	Fe	Si	P	Ca	Al	Hf	C	S	Other
TiO ₂	77.7	21.2	0.4	0.2	0.1	0.1	0.1	0.1	-	-	<0.1 ^a
C-NPTs	-	-	-	-	-	-	-	-	99.6	0.3	<0.1 ^b

^a - Cr, Cu
^b - Ca, Si, V, Al, Fe, P, Ti, Ni, Cu, K

**Figure 1** FTIR spectra of TiO₂ NPTs (a) and C-NPTs (b): ATR (a), transmission mode (KBr pellet) (b).**Figure 2** TGA (black), DSC (red) and DTA (blue) curves of TiO₂ NPTs (N₂, 20 °C/min).

Thus, Fe₂O₃ NPTs in water, 5 and 50 mmol/L SDS solutions have low stability (Figure S3). This affects the non-equilibrium particle size distributions and sedimentation in 30 min, which prevents further observations. At the same time, in 10 mmol/L SDS solution (Figure S3, c), the dispersions had a stable bimodal size distribution with modal diameters of 0.16 and 2.29 μm.

Al₂O₃ NPTs in both water and SDS solutions form aggregates with similar wide polymodal size distributions ranging from 20 nm to 160 μm (Figure S4). This suggests a

weak or absent interaction between the NPTs and the surfactants. In all cases, Al₂O₃ NPTs as well as Fe₂O₃ NPTs showed low stability and precipitated in 30 min of measurements.

The system of TiO₂ particles in water was variable and tended to equilibrium throughout the entire measurement (Figure 3). In one hour, two fractions of particles with modal diameters of 0.4 and 24.9 μm were formed. The IFT measurements showed (Table 2) that TiO₂ NPTs effectively reduce the interfacial tension at the *n*-hexane-water interface by two times. However, in SDS solutions, the stabilization of NPTs was observed during the entire hour of measurements. Practically monomodal size distributions with a modal diameter of ~0.4 μm are formed. With increasing SDS concentration, the fraction of aggregates with sizes of 1~10 μm slightly increases, which is probably also related to some increase in hydrophobicity of NPTs due to higher adsorption of surfactant.

β-Bi₂O₃ NPTs in water form large aggregates ~90 μm (Figure S5). However, in SDS solutions as well as for TiO₂ the stabilization of NPTs occurs. The aggregates are formed mainly with bimodal size distributions with fractions of ~0.18 and ~6.94 μm.

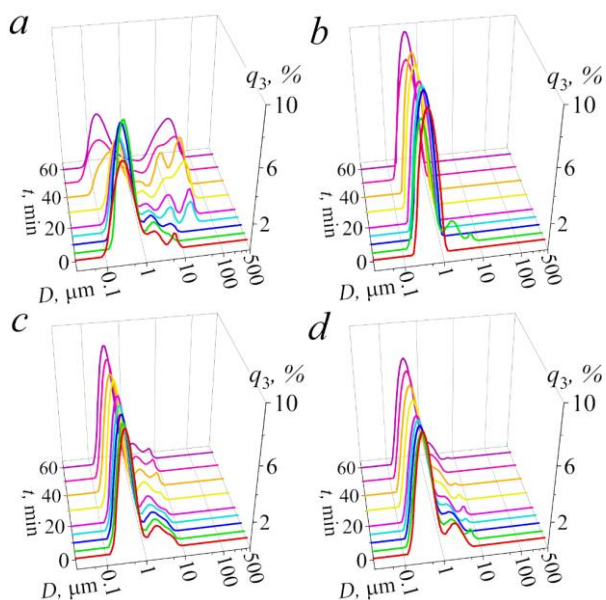
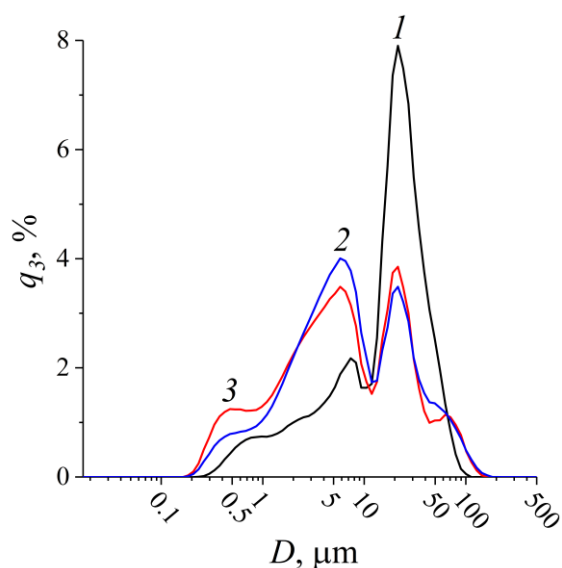
The aggregation of nanoparticles depends on both their type and method of synthesis. Different synthesis methods produce nanoparticles not only with different dispersions, but also with different surface properties. For example, the number of hydroxyl -OH groups on the particle surface may differ, which can have a critical impact on the adsorption of surfactants on NPTs. Apparently, TiO₂ and β-Bi₂O₃ particles have a higher affinity for SDS than other particles. Also, these nanoparticles simultaneously showed small aggregates (up to 0.18 μm) in SDS solutions and high stability. Therefore, TiO₂ and β-Bi₂O₃ nanoparticles were selected for further studies on the effect of pH on their aggregation.

3.3. Influence of surfactant on carbon nanoparticle aggregation

Carbon nanoparticles are of great interest because they are significantly more hydrophobic than oxide nanoparticles. C-NPTs are poorly wetted by water, which makes it difficult to disperse them. The obtained values of interfacial tension in the aqueous dispersion of C-NPTs (Table 2) confirm their hydrophobicity. In surfactant solutions, the particles disperse much better, which was proved experimentally (Figure 4). Size distributions of NPTs in all cases are polymodal with sizes from 0.18 to ~100 μm.

Table 2 Interfacial tension (IFT) measurements (between *n*-hexane and water dispersion).

Sample	IFT, mN/m
water	37.77±0.03
TiO ₂	19.31±0.03
C-NPts	38.78±0.05

**Figure 3** Size distribution of TiO₂ NPts aggregates: in water (a), in 5 mmol/L SDS (b); in 10 mmol/L SDS (c); in 50 mmol/L SDS (d) (q_3 – volume percentage, D – particle diameter).**Figure 4** Size distribution of C-NPts aggregates: in water (1), in 5 mmol/L SDS (2), in 50 mmol/L SDS (3) (q_3 – volume percentage, D – particle diameter).

However, in water the fraction with the modal diameter of 21.8 μm prevails, while in the SDS solutions the content of particles with sizes smaller than 12.0 μm significantly increases. The median particle size in water was 17.9 μm , and in 5 and 50 mmol/L SDS solutions – 5.6 and 6.1 μm , respectively. The surfactant solution expectedly stabilizes the C-NPts in the aqueous system. The modification of C-NPts with surfactant is promising because, unlike oxide

NPts, surfactant is adsorbed by orienting tails to the particle surface.

3.4. Influence of pH on nanoparticle aggregation

Hydroxyl groups and their amount on the surface of nanoparticles can affect the adsorption of ionogenic surfactants. Thus, hydroxyl groups are protonated in acidic medium, which should increase the adsorption of anionic surfactants, while in an alkaline medium, on the contrary, they dissociate, and the adsorption should decrease. Therefore, the pH of the system can have a significant influence on the adsorption of surfactants.

A study of the influence of pH on the aggregation of TiO₂ NPts showed that the size of the aggregates significantly depended on the pH (Figure 5a). The size (median D) of the aggregates of TiO₂ NPts in the water dispersion (without a buffer solution and SDS) was 196 nm. In the SDS solution (without buffer), the aggregate size increases ~ 1.6 times, which, as mentioned earlier, can be attributed to an increase in the hydrophobicity of the NPts surface due to surfactant adsorption. The smallest aggregates (165–177 nm) are formed in solutions with pH from 5.0 to 6.5. In an acidic medium, there is a sharp increase in TiO₂ aggregates up to ~ 900 nm, which seems to be due to the protonation of hydroxyl groups on the surface of NPts and a significant increase in surfactant aggregation. At $\text{pH} > 7.0$, the aggregate size also increases (up to 650 nm). In this case, in contrast with acidic media, this may be due to an increase in the negative charge of SDS, which leads to an increase in its adsorption on the surface of TiO₂ NPts in an alkaline medium. Thus, the pH range of 5.0–6.5 is optimal for obtaining stable TiO₂ nano-sols.

For TiO₂-BK NPts, it can be noted that the aggregate size decreases to 850 nm in the 5 mmol/L SDS (without buffer) compared to 1000 nm in the aqueous dispersion (Figure 5b). In an acidic medium ($\text{pH} < 2$), there is also a sharp enlargement of the aggregates up to 1360 nm. At $\text{pH} > 2$, the size of the aggregates is in most cases even smaller (up to 750 nm) than in the solution without the added buffer. However, the minimum size of the aggregates is still 4.6 times larger than that for TiO₂ NPts.

β -Bi₂O₃ NPts formed very large aggregates > 1200 nm (Figure 5, c). Moreover, in water (without a buffer), the aggregates had the smallest size (1210 nm), but in the SDS solution, aggregates of 1690 nm were formed. It is also remarkable that in all pH ranges except pH 3 larger aggregates were formed compared to the aqueous dispersion of β -Bi₂O₃ NPts.

The obtained results are in agreement with the zeta-potential measurements (Figure 6). The zeta-potential of TiO₂ NPts confirms the stability of the nano-sol in the region of 4.5 to 7.5 pH. When the particle size is changed (TiO₂-BK), the sol stabilizes in an alkaline environment (10–11 pH) in SDS solution. β -Bi₂O₃ NPts form stable sols in SDS solution at pH 2 and 10–12, which seems to be related to their ionization in strongly acidic and strongly alkaline media.

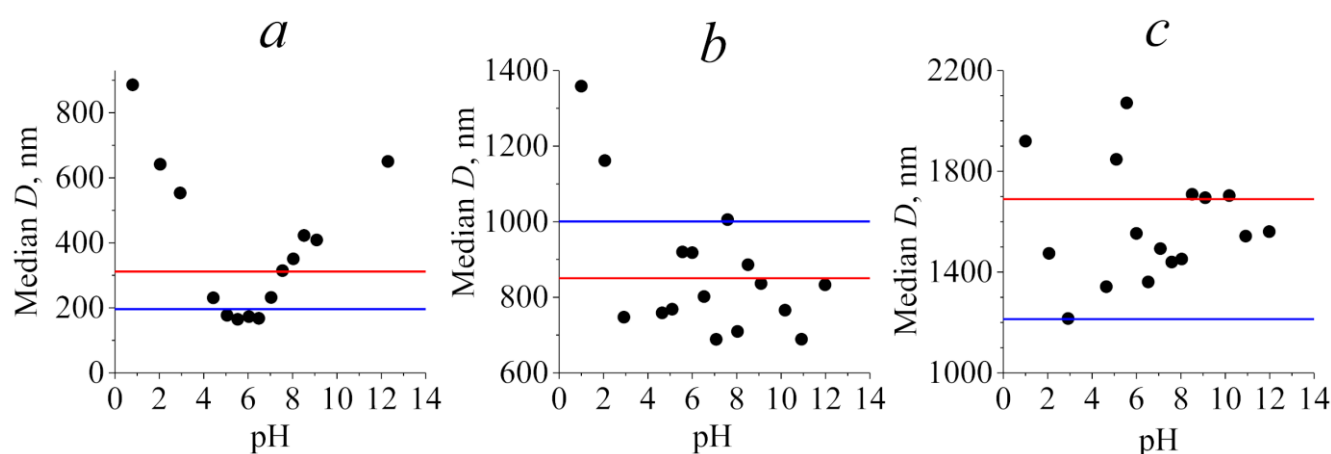


Figure 5 Dependence of the median diameter of nanoparticle aggregates on pH in 5 mmol/L SDS: TiO₂ (a); TiO₂-BK (b); β -Bi₂O₃ (c) (red line – in SDS; blue line – in water).

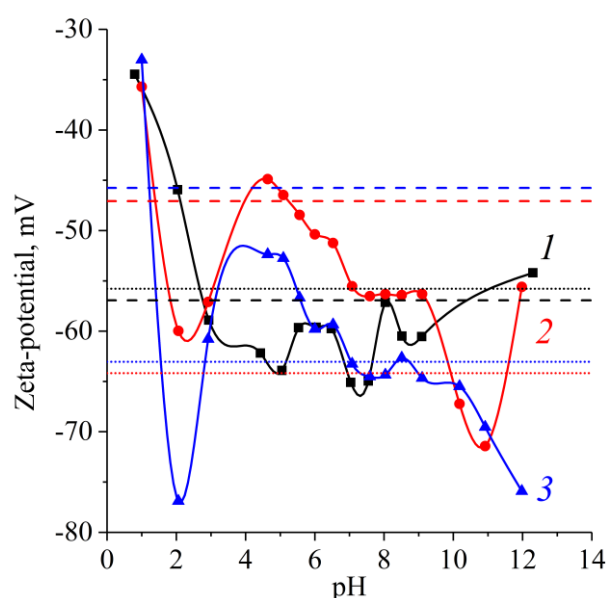


Figure 6 Zeta-potential measurements of TiO₂ (1, black), TiO₂-BK (2, red) and β -Bi₂O₃ (3, blue) NPs in pH-controlled solutions: dot lines – in 5 mmol/L SDS; dash lines – in water.

4. Limitations

The stability of nanoparticles in aqueous systems remains extremely critical. Even the smallest nanoparticles in water are prone to aggregation. Preventing or mitigating this phenomenon would be a big step in research.

5. Conclusions

In this work, the aggregation of oxide nanoparticles in water and sodium dodecyl sulfate solutions was studied by laser diffraction. TiO₂ and β -Bi₂O₃, obtained by plasma dynamic synthesis and by thermal decomposition of BiC₂H₄(OH), respectively, stabilized in anionic surfactant solutions better than other nanoparticles and formed the smallest aggregates. Therefore, these nanoparticles were chosen for further studies.

In the study of aggregation of carbon nanoparticles, it was shown that they are well stabilized in sodium dodecyl

sulfate solutions. These nanoparticles are of great interest for further research due to their different nature from oxide nanoparticles and poor study in chemical enhanced oil recovery.

The influence of pH on the nanoparticle aggregation was studied by evaluating the aggregate sizes and zeta-potential measured using dynamic light scattering. It was shown that among all the studied nanoparticles TiO₂ formed aggregates of the smallest size, and for them it was possible to determine the optimal pH range at which the most stable sols are formed (5.0–7.0 pH).

TiO₂ and carbon nanoparticles are the most promising for further research, in particular, for their modification with sodium dodecyl sulfate and further application in chemical enhanced oil recovery.

• Supplementary materials

This manuscript contains supplementary materials, which are available on the corresponding online page.

• Funding

The work was carried out within the framework of the state task of the ISSCM SB RAS (project №121032500065-5) and also was supported by the Russian Science Foundation (grant №22-13-20016), <https://www.rscf.ru/en>.

• Acknowledgments

The authors are grateful to Pavel Vadimovich Povalyaev (Tomsk Polytechnic University) for the provided carbon nanoparticles and Yurii Mikhailovich Yukhin (ISSCM SB RAN) for the provided β -Bi₂O₃ nanoparticles.

• Author contributions

Conceptualization: Yu.Yu.P., D.O.Z.
Formal Analysis: D.O.Z, A.V.K.
Funding acquisition: Y.G.M., Yu.Yu.P.
Investigation: D.O.Z, A.V.K.

Methodology: D.O.Z., Yu.Yu.P.

Project administration: Yu.Yu.P., A.N.Ch.

Resources: Yu.Yu.P., I.I.Sh., A.Ya.P.

Supervision: Yu.Yu.P.

Validation: A.V.K.

Visualization: D.O.Z., A.V.K.

Writing – original draft: D.O.Z., Yu.Yu.P.

Writing – review & editing: A.A.I., Y.G.M.

● Conflict of interest

The authors declare no conflict of interest.

● Additional information

Authors IDs:

Yuliya Yu. Petrova, Scopus ID [6603754153](#);

Anastasia A. Ivanova, Scopus ID [57196971233](#);

Alexey N. Cheremisin, Scopus ID [57193064808](#);

Ivan I. Shanenkov, Scopus ID [55543055400](#);

Alexander Ya. Pak, Scopus ID [37059570300](#);

Yuliya G. Mateyshina, Scopus ID [6506782050](#).

Websites:

Surgut State University, <https://int.surgu.ru/>;

Skoltech, <https://www.skoltech.ru/en/>;

Tyumen State University, <https://www.utmn.ru/en/>;

Tomsk Polytechnic University, <https://tpu.ru/en/>;

Institute of Solid State Chemistry and Mechanochemistry, Siberian Branch of the Russian Academy of Sciences, <http://www.solid.nsc.ru/en/>.

References

- Alsaba MT, Al Dushaishi MF, Abbas AK. A comprehensive review of nanoparticles applications in the oil and gas industry. *J Pet Explor Prod Technol.* 2020;10(5):1389–1399. doi:[10.1007/s13202-019-00825-z](#)
- Franco CA, Zabala R, Cortés FB. Nanotechnology applied to the enhancement of oil and gas productivity and recovery of Colombian fields. *J Pet Sci Eng.* 2017;157:39–55. doi:[10.1016/j.petrol.2017.07.004](#)
- Chen L, Zhu X, Wang L, Yang H, Wang D, Fu M. Experimental study of effective amphiphilic graphene oxide flooding for an ultralow-permeability reservoir. *Energy Fuels.* 2018;32(11):11269–11278. doi:[10.1021/acs.energyfuels.8b02576](#)
- Goshtasp C. Effect of nano titanium dioxide on heavy oil recovery during polymer flooding. *Petroleum Sci Technol.* 2016;34(7):633–641. doi:[10.1080/10916466.2016.1156125](#)
- Dai C, Li H, Zhao M, Wu Y, You Q, Sun Y, Zhao G, Xu K. Emulsion behavior control and stability study through decorating silica nano-particle with dimethyldodecylamine oxide at n-heptane/water interface. *Chem Eng Sci.* 2018;179:73–82. doi:[10.1016/j.ces.2018.01.005](#)
- Eltoum H, Yang YL, Hou JR. The effect of nanoparticles on reservoir wettability alteration: a critical review. *Petroleum Sci.* 2021;18:136–153. doi:[10.1007/s12182-020-00496-0](#)
- Karimi A, Fakhroueian Z, Bahramian A, Khiabani NP, Darabad JB, Azin R, Arya S. Wettability alteration in carbonates using zirconium oxide nanofluids: EOR Implications. *Energy Fuels.* 2012;26(2):1028–1036. doi:[10.1021/ef201475u](#)
- Fan H, Striolo A. Nanoparticle effects on the water-oil interfacial tension. *Phys Rev E.* 2012;86(5):051610. doi:[10.1103/PhysRevE.86.051610](#)
- Almahfood M, Bai B. The synergistic effects of nanoparticle-surfactant nanofluids in EOR applications. *J Petroleum Sci Eng.* 2018;171:196–210. doi:[10.1016/j.petrol.2018.07.030](#)
- Zhong X, Li C, Li Y, Pu H, Zhou Y, Zhao J. Enhanced oil recovery in high salinity and elevated temperature conditions with a zwitterionic surfactant and silica nanoparticles acting in synergy. *Energy Fuels.* 2020;34(3):2893–2902. doi:[10.1021/acs.energyfuels.9b04067](#)
- Arab D, Kantzas A, Bryant SL. Nanoparticle stabilized oil in water emulsions: A critical review. *J Pet Sci Eng.* 2018;163:217–242. doi:[10.1016/j.petrol.2017.12.091](#)
- Behzadi A, Mohammadi A. Environmentally responsive surface-modified silica nanoparticles for enhanced oil recovery. *J Nanopart Res.* 2016;18:1–19. doi:[10.1007/s11051-016-3580-1](#)
- Ngouangna EN, Manan MA, Oseh JO, Norddin MNA, Agi A, Gbadamosi AO. Influence of (3-Aminopropyl) triethoxysilane on silica nanoparticle for enhanced oil recovery. *J Mol Liquids.* 2020;315:113740. doi:[10.1016/j.molliq.2020.113740](#)
- Zhao T, Chen J, Chen Y, Zhang Y, Peng J. Study on synergistic enhancement of oil recovery by halloysite nanotubes and glucose-based surfactants. *J Dispersion Sci Technol.* 2021;42:934–946. doi:[10.1080/01932691.2020.1721297](#)
- Son HA, Lee T. Enhanced oil recovery with size-dependent interactions of nanoparticles surface-modified by zwitterionic surfactants. *Appl Sci.* 2021;11(16):7184. doi:[10.3390/app11167184](#)
- Ahmed A, Saaid IM, Ahmed AA, Pilus RM, Baig MK. Evaluating the potential of surface-modified silica nanoparticles using internal olefin sulfonate for enhanced oil recovery. *Pet Sci.* 2019;17:722–733. doi:[10.1007/s12182-019-00404-1](#)
- Pal N, Verma A, Ojha K, Mandal A. Nanoparticle-modified gemini surfactant foams as efficient displacing fluids for enhanced oil recovery. *J Mol Liquids.* 2020;310:113193. doi:[10.1016/j.molliq.2020.113193](#)
- Venancio JCC, Nascimento RSV, Perez-Gramatges A. Colloidal stability and dynamic adsorption behavior of nanofluids containing alkyl-modified silica nanoparticles and anionic surfactant. *J Mol Liquids.* 2020;308:1–7. doi:[10.1016/j.molliq.2020.113079](#)
- Moghadam TF, Azizian S, Wettig S. Synergistic behaviour of ZnO nanoparticles and gemini surfactants on the dynamic and equilibrium oil/water interfacial tension. *Phys Chem Chem Phys.* 2015;17(11):1–8. doi:[10.1039/C5CP00510H](#)
- Pillai P, Sawa RK, Singha R, Padmanabhan E, Mandal A. Effect of synthesized lysine-grafted silica nanoparticle on surfactant stabilized O/W emulsion stability: Application in enhanced oil recovery. *J Pet Sci Eng.* 2019;177:861–871. doi:[10.1016/j.petrol.2019.03.007](#)
- Saigal T, Dong H, Matyjaszewski K, Tilton RD. Pickering Emulsions Stabilized by Nanoparticles with Thermally Responsive Grafted Polymer Brushes. *Langmuir.* 2010;26(19):15200–15209. doi:[10.1021/la1027898](#)
- Dai C, Li H, Zhao M, Wu Y, You Q, Sun Y, Zhao G, Xu K. Emulsion behavior control and stability study through decorating silica nano-particle with dimethyldodecylamine oxide at n-heptane/water interface. *Chem Eng Sci.* 2018;179:73–82. doi:[10.1016/j.ces.2018.01.005](#)
- Omran M, Akarri S, Torsaeter O. The effect of wettability and flow rate on oil displacement using polymer-coated silica nanoparticles: a microfluidic study. *Proces.* 2020;8(8):991. doi:[10.3390/pr8080991](#)
- Mishchenko KV, Gerasimov KB, Yukhin YM. Thermal decomposition of some bismuth oxocarboxylates with formation of β -Bi₂O₃. *Mater Today Proc.* 2020;25(3):391–394. doi:[10.1016/j.matpr.2019.12.102](#)
- Pak AY, Povalyaev PV, Frantsina EV, Grinko AA, Petrova YY, Arkachenkova VV. Obtaining carbon graphite-like nanomaterials in asphaltene-based waste recycling. *Bulletin of the*

- Tomsk Polytechnic University. *Geo Assets Eng.* 2022;333(12):25-36.
26. Sivkov A, Vympina Y, Ivashutenko A, Rakhmatullin I, Shanenkova Y, Nikitin D, Shanenkov I. Plasma dynamic synthesis of highly defective fine titanium dioxide with tunable phase composition. *Ceram Int.* 2022;48(8):10862-10873. doi:[10.1016/j.ceramint.2021.12.303](https://doi.org/10.1016/j.ceramint.2021.12.303)
27. Viades-Trejo J, Gracia-Fadrique J. Spinning drop method: From Young-Laplace to Vonnegut. *Colloids Surfaces A Physicochem Eng Aspects.* 2007;302(1-3):549-552. doi:[10.1016/j.colsurfa.2007.03.033](https://doi.org/10.1016/j.colsurfa.2007.03.033)
28. Cao Y, Zhao RH, Zhang L, Xu ZC, Jin ZQ, Luo L, Zhang L, Zhao S. Effect of electrolyte and temperature on interfacial tensions of alkylbenzene sulfonate solutions. *Energy Fuels.* 2012;26(4):2175-2181. doi:[10.1021/ef201982s](https://doi.org/10.1021/ef201982s)
29. Sharma S, Reddy AVD, Jayarambabu N, Kumar NVM, Saineeetha A, Rao KV, Kailasa S. Synthesis and characterization of Titanium dioxide nanopowder for various energy and environmental applications. *Mater Today Proc.* 2020;26(1):158-161. doi:[10.1016/j.matpr.2019.09.203](https://doi.org/10.1016/j.matpr.2019.09.203)